Inorganic Chemistry

Article

pubs.acs.org/IC

Highly Efficient Near-Infrared-Emitting Lanthanide(III) Complexes Formed by Heterogeneous Self-Assembly of Ag^{I}, Ln^{III}, and Thiacalix[4]arene-*p*-tetrasulfonate in Aqueous Solution (Ln^{III} = Nd^{III}, Yb^{III})

Nobuhiko Iki,*[,†] Shouichi Hiro-oka,[†] Teppei Tanaka,[†] Chizuko Kabuto,[‡] and Hitoshi Hoshino[†]

[†]Graduate School of Environmental Studies and [‡]School of Engineering, Tohoku University, 6-6-07 Aramaki-Aoba, Aoba-ku, Sendai 980-8579 Japan

Supporting Information

ABSTRACT: Heterogeneous self-assembly of thiacalix[4]-arene-*p*-tetrasulfonate (TCAS), Ag^{I}, and Ln^{III} (= Nd^{III}, Yb^{III}) in aqueous solutions conveniently afforded ternary complexes emitting Ln^{III}-centered luminescence in the near-infrared (NIR) region. A solution-state study revealed that the Ag^{I}-Nd^{III}-TCAS system gave a complex $Ag^{I}_4{\cdot}Nd^{III}{\cdot}TCAS_2$ in a wide pH range of 6−12. In contrast, the Ag^{I}-Yb^{III}-TCAS system gave $Ag^{I}_2{\cdot}Yb^{III}_2{\cdot}TCAS_2$ at a pH of around 6 and $Ag^{I}_2{\cdot}Yb^{III}{\cdot}TCAS_2$ at a pH of approximately 9.5. The structures of the Yb^{III} complexes were proposed based on comparison with known Ag^{I}-Tb^{III}-TCAS complexes that show the same self-assembly behavior. In $Ag^{I}_2{\cdot}Yb^{III}_2{\cdot}TCAS_2$, two TCAS ligands sandwiched a cyclic array of a Ag^{I}−Ag^{I}−Yb^{III}−Yb^{III} core. In $Ag^{I}_2{\cdot}Yb^{III}{\cdot}TCAS_2$, Yb^{III} was accommodated in an O_8 cube consisting of eight phenolate O^- groups from two TCAS ligands linked by two S−Ag−S linkages. Crystallographic analysis of $Ag^{I}_4{\cdot}Nd^{III}{\cdot}TCAS_2$ revealed that the structure was similar to $Ag^{I}_2{\cdot}Yb^{III}{\cdot}TCAS_2$ but that it had four instead of two S−Ag−S linkages. The number of water molecules coordinating to Ln^{III} (q) estimated on the basis of the luminescent lifetimes was as follows: $Ag^{I}_4{\cdot}Nd^{III}{\cdot}TCAS_2$, 0; $Ag^{I}_2{\cdot}Yb^{III}_2{\cdot}TCAS_2$, 2.4; and $Ag^{I}_2{\cdot}Yb^{III}{\cdot}TCAS_2$, 0. These findings were compatible with the solution-state structures. The luminescent quantum yield (Φ) for $Ag^{I}_4{\cdot}Nd^{III}{\cdot}TCAS_2$ was 4.9×10^{-4}, which is the second largest value ever reported in H_2O. These findings suggest that the O_8 cube is an ideal environment to circumvent deactivation via O−H oscillation of coordinating water. The Φ values for $Ag^{I}_2{\cdot}Yb^{III}_2{\cdot}TCAS_2$ and $Ag^{I}_2{\cdot}Yb^{III}{\cdot}TCAS_2$ were found to be 3.8×10^{-4} and 3.3×10^{-3}, respectively, reflecting the q value. Overall, these results indicate that the ternary systems have the potential for a noncovalent strategy via self-assembly of the multidentate ligand, Ln^{III}, and an auxiliary metal ion to obtain a highly efficient NIR-emissive Ln^{III} complex that usually relies on elaborate covalent linkage of a chromophore and multidentate ligands to expel coordinating water.

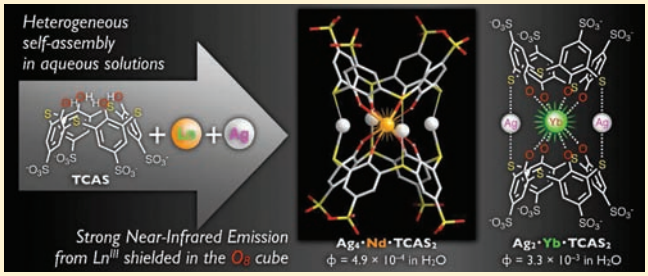

INTRODUCTION

Transparency of biotissues in the near-infrared (NIR) region (650−1000 nm) has resulted in the attention of designers of luminescent bioprobes shifting from visible to NIR-emissive chemical motifs.[1,2] In this context, the design of an NIR-emissive lanthanide(III) (Ln^{III} such as Nd^{III}, Yb^{III}, and Er^{III}) complex should have a great impact in this field owing to the advantages associated with their facile recognizable spectra, which have large Stokes shifts and sharp emission bands, as well as their long emission lifetimes, which enable time-resolved detection; these advantages are not exhibited by organic dyes.[3,4] In general, design of ligands for such Ln^{III} complexes relies on a covalent strategy, namely, covalent joining of a chromophore and multidentate ligand. The chromophore is responsible for the absorption of photons to excite the Ln^{III} center, while the multidentate ligand plays a vital role in protecting the Ln^{III} center from solvent water with the ability to de-excite the Ln^{III} center through high vibration energy of the O−H stretching. This is particularly true for Nd^{III}, Yb^{III}, and Er^{III}, which have a small f-f energy gap. In accordance with this strategy, ligands affording highly luminescent Nd^{III} complexes have been reported. For example, Korovin et al. reported that ligand **1** derived from 1,10-phenanthroline with two aza-macrocyclic ligands formed a dineodymium(III) complex ($Nd^{III}_2{\cdot}$**1**, Scheme 1) with the highest luminescence quantum yield ($\Phi = 8.5 \times 10^{-4}$) ever reported for aqueous solutions.[5] Imbert et al. recently reported that tetrakis(8-hydroxyquinolinate)podand **2** formed a Nd^{III} complex ($Nd^{III}{\cdot}$**2**) with $\Phi = 4.0 \times 10^{-4}$.[6] Despite the clarity of the covalent strategy to prepare these ligands, its synthesis is laborious, requires many steps, and produces only a low yield of the final product. For example, ligand **2** was synthesized with 2% yield over five steps.[6] In addition, Korovin did not provide the total yield of ligand **1**, but did report that its

Received: September 6, 2011
Published: January 24, 2012

dx.doi.org/10.1021/ic2019583 | Inorg. Chem. 2012, 51, 1648−1656

Scheme 1

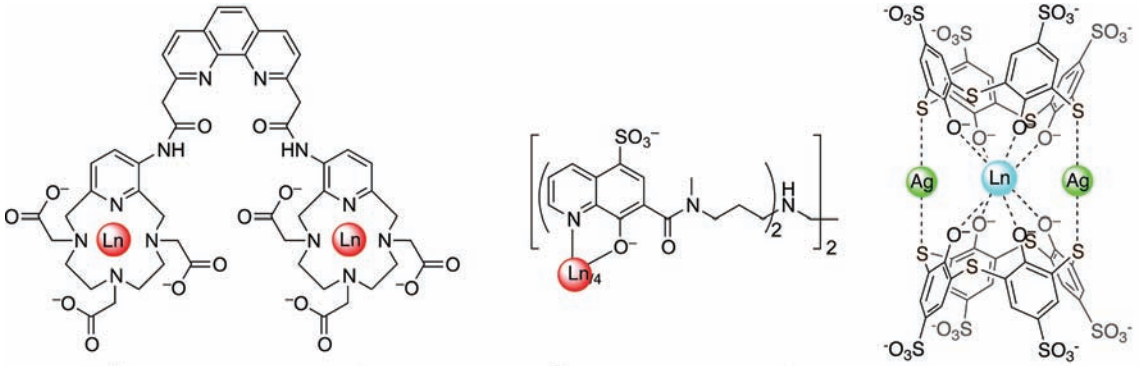

synthesis was quite complex.[5] Accordingly, an alternative to the covalent strategy is necessary to achieve a breakthrough in the preparation of NIR-emissive Ln^{III} complexes.

Since we found the facile one-step synthesis of thiacalix[4]-arene (TCA) with an acceptable yield (54%),[7] we have engaged in studying the functions arising from the sulfide moiety.[8] To facilitate the solubilization in water, TCA was conveniently sulfonated to afford thiacalix[4]arene-*p*-tetrasulfonate (TCAS, 69% yield) to open the way to pursue complexation study with Ln^{III} in aqueous solutions.[9,10] We recently found that simple mixing of Ag^{I}, Tb^{III}, and TCAS in aqueous solutions afforded heterogeneous self-assembly of a luminescent ternary complex, Ag^{I}_2·Tb^{III}·$TCAS_2$ (**3**).[11] This complex provided the Tb^{III} center with an O_8-cubic coordination environment that contained eight phenolate O^- groups to expel coordinating water,[12] which led to an exceptionally long emission lifetime in aqueous solutions (4.6 ms).[11,13] The water-free coordination environment provided by the self-assembly inspired us to produce NIR-emissive complexes using Ln^{III} such as Nd^{III} and Yb^{III} in place of Tb^{III}. Here, we report the self-assembly of Ag^{I}-Nd^{III}-TCAS and Ag^{I}-Yb^{III}-TCAS ternary complexes in aqueous solutions, as well as their structure and photophysical properties to demonstrate their potential for a noncovalent strategy that employs heterogeneous assembly of the ternary components in the design of NIR-emissive complexes.

EXPERIMENTAL SECTION

Materials. Tetrasodium thiacalix[4]arene-*p*-tetrasulfonate (TCAS) was synthesized as previously reported[10] and stocked as an aqueous solution of 0.01 M. Stock solutions of 0.01 M Nd^{III}, Yb^{III}, and Gd^{III} were prepared by dissolving nitrate hexahydrate (99.5% purity each) purchased from Wako Pure Chemical Industries, Ltd. (Osaka) into 0.01 M HNO_3 solution. A stock solution of 0.01 M Ag^{I} was prepared by dissolving $AgNO_3$ (99.8%, Kanto Chemical Company, Inc., Tokyo) in 0.01 M HNO_3. The concentration of the metal ion in the stock solutions was determined using accepted chelatometry.[14] The pH buffers 2-morphorinoethanesulfonic acid (MES), 2-[4-(2-hydroxyethyl)-1-piperazinyl]ethanesulfonic acid (HEPES), *N*-cyclohexyl-2-aminoethanesulfonic acid (CHES), and *N*-cyclohexyl-3-aminopropanesulfonic acid (CAPS) were purchased from Dojindo Laboratories, Kumamoto. Tris(hydroxymethyl)aminomethane (Tris) was purchased from Nacalai Tesque, Inc., Kyoto. Buffer solution (0.5 M) was prepared by dissolving the buffer in water, adjusting the pH with HNO_3 or NaOH and then diluting the solutions to the appropriate volume with water. The pH ranges of the buffers used were as follows: MES/NaOH (pH 5.5−6.6), BES/NaOH (pH 6.6−7.5), HEPPSO/NaOH (pH 7.5−8.6), CHES/NaOH (pH 8.6−10.0), and CAPS/NaOH (pH 10.0−11.0). 4′,5′-Bis[*N*,*N*-bis(carboxymethyl)-aminomethyl]fluorescein (Calcein) was purchased from Fluka and used as 1 mM solution dissolved in 0.1 M Tris buffer solution (pH = 8.3). All other chemicals used were of guaranteed ultrapure grade. Heavy water D_2O (99.8 atom % D) was purchased from Acros Organics (Geel, Belgium). Double distilled water was used throughout this study unless otherwise noted.

Equipment. A Jobin Yvon FluoroLog-3 model FL3-11 spectrofluorometer equipped with a 450 W Xe lamp as the excitation source and an InGaAs semiconductor detector (DSS-IGA020L) was used to record the luminescence spectra. The luminescence lifetime was measured using a Unisoku TSP-2000 time-resolved spectrophotometer, in which an Nd:YAG laser with quadrupled frequency (266 nm) acted as the excitation source. The pH was recorded using a TOA HM-25R pH meter with a combined glass electrode. Electro-spray ionization-mass spectrometry was conducted using a Fourier transform ion cyclotron resonance (FTICR) mass spectrometer APEX III (Bruker). The mass spectra were simulated using the software iMass for Mac OS X ver. 1.1.[15]

Measurement. Ternary complexes were prepared by simply mixing appropriate amounts of aqueous solutions of Ag^{I}, Ln^{III}, TCAS, and pH buffer. Prior to measurement of the absorption, luminescence, and mass spectra, the sample solution was allowed to stand for 1 h at room temperature to ensure equilibration. The overall luminescence quantum yields were estimated as previously described[10] using a calcein complex of Nd^{III} or Yb^{III} as the standard.[16] The number of water molecules coordinating to the Nd^{III} and Yb^{III} center were estimated by using Horrock's eqs 1[17] and 2,[18] respectively, with the lifetimes (τ) measured in H_2O and D_2O (>99% D) solutions as follows:

$$q = A(\Delta k_{obs}) - B \quad (1)$$

$$q = C(\Delta k_{obs} - D) \quad (2)$$

where A = 130 ns, B = 0.4, C = 1 μs, D = 0.2 μs^{-1}, and Δk_{obs} is the difference in the emission rate in H_2O and D_2O as given by eq 3.

$$\Delta k_{obs} = 1/\tau_{H2O} - 1/\tau_{D2O} \quad (3)$$

Preparation of Single Crystals of Ag^{I}_4·Nd^{III}·$TCAS_2$. Nd-$(NO_3)_3$·$6H_2O$ (94.6 mg, 5.1 × 10^{-5} mol), Ag_2SO_4 (34.9 mg, 1.1 × 10^{-4} mol), and about 2 mL of water were added to a small beaker, allowed to dissolve, and mixed thoroughly under ultrasonication. In another small beaker, TCAS (94.6 mg, 1.05 × 10^{-4} mol), 2 mL of MES buffer (0.1 M), and an appropriate amount of 1.0 M NaOH were added to adjust the pH to 5.9 (as determined using a pH meter). Next, the Ag^{I}−Nd^{III} mixed solution was added dropwise to the TCAS solution while maintaining the pH at 5.9 by occasional dropwise addition of 1.0 M NaOH. The final volume of the solution was about 10 mL. Finally, a 1 mL aliquot of this mixture was transferred into a small cuvette, which was subsequently placed in a large vial half-filled with DMF. The vial was then sealed and allowed to stand for about

dx.doi.org/10.1021/ic2019583 | Inorg. Chem. 2012, 51, 1648−1656

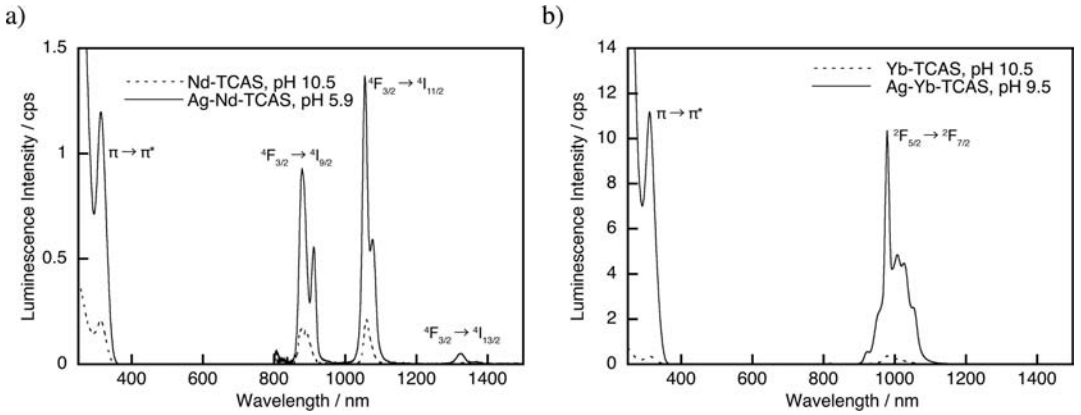

Figure 1. Excitation and emission spectra of solution containing Ln^{III}-TCAS binary and Ag^{I}-Ln^{III}-TCAS ternary components (Ln^{III} = (a) Nd^{III}, (b) Yb^{III}). Conditions: $[Ln^{III}] = 5 \times 10^{-6}$ M, $[Ag^{I}] = 0$ or 1.0×10^{-5} M, [TCAS] = 5.0 or 10.0×10^{-6} M, [Buffer] = 2.0×10^{-3} M, λ_{ex} = 312 nm, λ_{em} = (a) 1059 and (b) 978 nm.

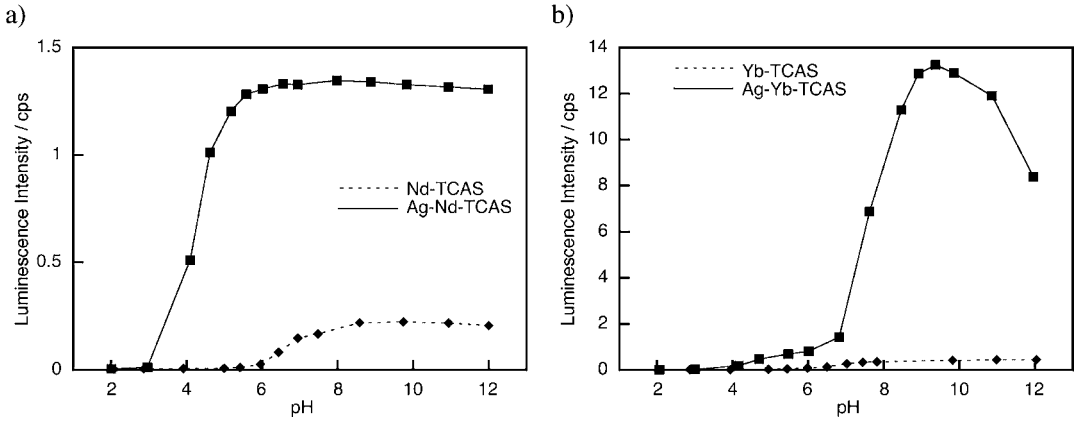

Figure 2. pH dependence of luminescence intensity for the Ln^{III}-TCAS binary and Ag^{I}-Ln^{III}-TCAS ternary systems (Ln^{III} = (a) Nd^{III}, (b) Yb^{III}). Conditions: (a) Nd^{III}-TCAS binary, $[Nd_{III}] = 5.0 \times 10^{-6}$ M, [TCAS] = 5.0×10^{-6} M, [Buffer] = 1.0×10^{-3} M; Ag^{I}-Nd^{III}-TCAS ternary, $[Nd_{III}] = 5.0 \times 10^{-6}$ M, $[Ag_{I}] = 2.0 \times 10^{-5}$ M, [TCAS] = 10.0×10^{-6} M, [Buffer] = 1.0×10^{-3} M. λ_{ex} = 312, λ_{em} = 1059 nm, (b) Yb^{III}-TCAS binary, $[Yb_{III}] = 5.0 \times 10^{-6}$ M, [TCAS] = 5.0×10^{-6} M, [Buffer] = 1.0×10^{-3} M; Ag^{I}-Yb^{III}-TCAS ternary, $[Yb_{III}] = 5.0 \times 10^{-6}$ M, $[Ag_{I}] = 1.0 \times 10^{-5}$ M, [TCAS] = 10.0×10^{-6} M, [Buffer] = 1.0×10^{-3} M. λ_{ex} = 312, λ_{em} = 978 nm.

one month. This process led to production of colorless blocks of $Na_9{\cdot}[Ag_4{\cdot}Nd{\cdot}TCAS_2]{\cdot}8dmf{\cdot}6H_2O$ (3 mg, ca. 30% yield).

Crystal Data. $Na_9{\cdot}[Ag_4{\cdot}Nd{\cdot}TCAS_2]{\cdot}8dmf{\cdot}6H_2O$ ($C_{72}H_{92}Ag_4N_8Na_9O_{50}S_{16}Nd$; M_r = 3165.13): colorless prism, triclinic, space group $P\bar{1}$, a = 11.8384(15), b = 13.7457(17), c = 17.587(2) Å, α = 72.5520(10), β = 85.3630(10), γ = 87.7210(10)°, V = 2720.9(6) Å^3, Z = 1, T = 173(2) K, ρ_{calcd} = 1.932 g/cm^3, $F(000)$ = 1583, $\mu(Mo_{K\alpha})$ = 1.803 mm^{-1}. The data were collected using a Bruker APEX2 diffractometer ($Mo_{K\alpha}$ = 0.71073 Å). The structures were elucidated by direct methods using SHELXS-97[19,20] and then further refined using least-squares on F^2, SHELXL-97, with 772 parameters, wR_2 = 0.0680 (12178 unique reflections), R_1 = 0.0240 (11705 reflections with $I > 2\sigma$). X-ray analysis was conducted using the free GUI software Yadokari-XG 2009.[21] CCDC-838840 contains the supplementary crystallographic data in support of the findings of this paper. These data can be obtained free of charge from the Cambridge Crystallographic Data Centre at www.ccdc.cam.ac.uk/data_request/cif.

RESULTS AND DISCUSSION

Luminescence Spectra. The excitation and emission spectra for the solution prepared by mixing the aqueous solutions of $AgNO_3$, $Nd(NO_3)_3$, TCAS, and pH buffer (pH = 5.9) showed ligand-centered absorption owing to a π–π^* transition at 312 nm and Nd^{III}-centered NIR emission at 874, 1059, and 1330 nm, respectively (Figure 1a). The large Stokes shift that was observed can be attributed to energy transfer from TCAS to the Nd^{III} center, suggesting formation of a complex species containing both Nd^{III} and TCAS. In addition, the Nd^{III}-TCAS binary mixture exhibited similar absorption and Nd^{III} emission, but with lower intensity, suggesting that coexistence of Ag^{I} should have led to the formation of a highly luminescent ternary complex. Moreover, the $^4F_{3/2} \rightarrow {}^4I_{9/2}$ and $^4F_{3/2} \rightarrow {}^4I_{11/2}$ emission bands showed different fine structures. Specifically, the ternary mixture showed splitting, but the binary mixture did not. Because splitting of the f-f transition bands (i.e., Stark splitting) is caused by the ligand field of the Ln^{III} center,[22−24] the coordination environments around the Nd^{III} center differ among binary and ternary complexes. These findings provide further evidence of the formation of ternary complex species.

The Ag^{I}-Yb^{III}-TCAS ternary system also exhibited excitation and emission spectra that could be assigned to the ligand-centered π–π^* transition and Yb^{III}-centered $^2F_{5/2} \rightarrow {}^2F_{7/2}$ emission, respectively (for pH = 9.5, see Figure 1b). Obviously, the intensity was much stronger than that attained with the Yb^{III}-TCAS binary system, suggesting that Ag^{I} played an indispensable role in formation of the highly emissive Ag^{I}-Yb^{III}-TCAS ternary complex. On the basis of these Nd^{III} and Yb^{III} systems, the ability of NIR-emissive Ag^{I}-Ln^{III}-TCAS ternary

dx.doi.org/10.1021/ic2019583 | Inorg. Chem. 2012, 51, 1648−1656

complexes to be formed by simply mixing the components was confirmed.

pH Dependence of Formation of the Complexes. The pH dependence of the intensity of the Nd^{III} emission at 1059 nm from the Nd^{III}-TCAS binary and Ag^{I}-Nd^{III}-TCAS ternary mixtures was investigated after equilibrating the mixtures for 1 h (Figure 2a). In the former case, the intensity increased at pH values greater than 6 and reached a plateau at pH 8, indicating the formation of a complex involving coordination of phenolate O^{-} formed by acid dissociation of the phenolic OH of TCAS at high pH. In contrast, the ternary system exhibited an increase at pH 4 and a plateau at pH > 5.9, with nearly 6 times higher intensity than that of the binary mixture. Notably, at pH 5.9, the binary mixture showed almost no luminescence, while the ternary mixture exhibited high luminescence. These findings indicate that Ag^{I} plays a role in the assembly of Nd^{III} and TCAS possibly via Ag−S bond formation. The large difference in the luminescence intensity in the plateau region for the binary and ternary complexes suggests that the luminescence efficiency of the ternary complex is higher than that of the binary one (vide infra).

In the Yb^{III}-TCAS binary system, the intensity increased at pH 6 (Figure 2b), which is similar to the results observed for the Nd^{III}-TCAS system. However, the Ag^{I}-Yb^{III}-TCAS ternary mixture exhibited different behavior. Specifically, in this mixture, the first increase was observed at pH 4.5, followed by a slight increase at pH 5−6. Following the second steep increase at pH 8, the intensity reached a maximum at pH 9.5, after which it gradually decreased. This two-step rise is indicative of the formation of two types of Ag^{I}-Yb^{III}-TCAS ternary complex species at pH values of around 5−6 and 9.5 depending upon the acid dissociation of the phenolic OH of the TCAS ligand. This behavior of the Ag^{I}-Yb^{III}-TCAS ternary system is very similar to the case of the Ag^{I}-Tb^{III}-TCAS ternary system providing ternary complexes $Ag^{I}_{2}\cdot Tb^{III}_{2}\cdot TCAS_{2}$ (Scheme 2) and $Ag^{I}_{2}\cdot Tb^{III}\cdot TCAS_{2}$ at pH values of around 6 and 10, respectively.[11] In addition, the gradual decrease that was observed at pH > 9.5 appeared to be caused by dissociation of the ternary complex via the formation of hydroxides of Yb^{III}. This was not observed for the Ag^{I}-Nd^{III}-TCAS system, reflecting the higher stability of the complex arising from the four S−Ag−S linkages to tightly bind two TCAS ligands to include the Nd^{III} core (vide infra). On the other hand, the Ag−Yb-TCAS ternary complex at high pH only has two S−Ag−S linkages to result in the lower stability.

Scheme 2

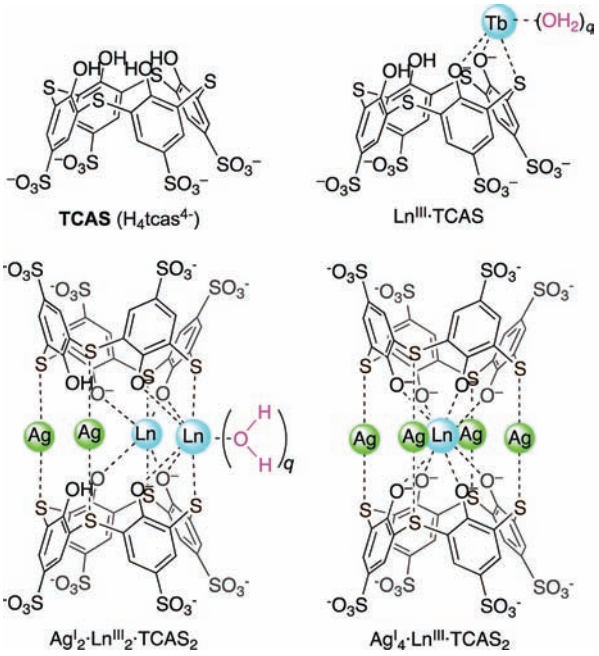

Structure of the Complexes in Solution. We first determined the stoichiometry of the ternary complexes using the molar ratio method and electro-spray ionization (ESI)-MS. In the Ag^{I}-Nd^{III}-TCAS system at pH 5.9, the luminescence intensity of the Nd^{III} center (at 1059 nm) was recorded while varying different ratios such as [TCAS]/[Nd^{III}] and [Ag^{I}]/[TCAS] (Supporting Information, Figure S1). On the basis of the clear inflection points, the Ag^{I}:Nd^{III}:TCAS ratio was estimated to be 4:1:2 in aqueous solutions. Furthermore, the ESI-mass spectrum obtained at pH 5.9 showed two main peaks that each contained the components Ag^{I}, Nd^{III}, and TCAS in the ratio of 4:1:2. For example, the intense peak at around m/z = 733.0334 could be assigned to $[4Ag^{+} + Nd^{3+} + 2TCAS^{8-} + 6H^{+}]^{3-}$ (m/z = 733.0306(calcd.)) using a simulation of the isotopomer peak pattern (Figure 3). Another peak at around m/z = 1100.0507(obs.) was attributed to $[4Ag^{+} + Nd^{3+} + 2TCAS^{8-} + 7H^{+}]^{2-}$ (m/z = 1100.0497(calcd.)) (Supporting Information, Figure S2). Thus, the results obtained using the molar ratio method and ESI-MS agreed well in that they unambiguously assigned the ternary species in the solutions as $Ag^{I}_{4}\cdot Nd^{III}\cdot TCAS_{2}$. Because the stoichiometry of the Ag^{I}-Tb^{III}-TCAS ternary complex varied with changing pH,[11] we also measured the ESI-MS of the Ag^{I}-Nd^{III}-TCAS ternary solution at pH 10.5 (Supporting Information, Figure S3). These measurements resulted in the same main peaks being assigned to $Ag^{I}_{4}\cdot Nd^{III}\cdot TCAS_{2}$: $[4Ag^{+} + Nd^{3+} + 2TCAS^{8-} + 6H^{+}]^{3-}$, m/z = 733.0331(obs.), 733.0306(calcd.) and $[4Ag^{+} + Nd^{3+} + 2TCAS^{8-} + 7H^{+}]^{2-}$, m/z = 1100.0536(obs.), 1100.0497-(calcd.). These findings confirm formation of the ternary complex $Ag^{I}_{4}\cdot Nd^{III}\cdot TCAS_{2}$ at pH values ranging from 6 to 12, as suggested by the intensity in the plateau region shown in Figure 2a. Among the Ag^{I}-Ln^{III}-TCAS ternary systems we have studied to date, the only species detected in aqueous solutions were $Ag^{I}_{2}\cdot Tb^{III}_{2}\cdot TCAS_{2}$ and $Ag^{I}_{2}\cdot Tb^{III}\cdot TCAS_{2}$.[11] Therefore, $Ag^{I}_{4}\cdot Nd^{III}\cdot TCAS_{2}$ provides the first example of a ternary complex containing four Ag^{I} atoms. In the solid state, the only known example of the 4:1:2 complex has been isolated as single crystals of $Ag^{I}_{4}\cdot Tb^{III}\cdot TCAS_{2}$[12] containing four S−Ag−S bridges to link the two TCAS ligands (Scheme 2). Accordingly, it can be assumed that $Ag^{I}_{4}\cdot Nd^{III}\cdot TCAS_{2}$ adopts the same structure as $Ag^{I}_{4}\cdot Tb^{III}\cdot TCAS_{2}$, having an O_{8}-cubic coordination environment. This was supported by X-ray analysis of the single crystal (vide infra).

In the case of the Yb^{III} system, the molar ratio method at pH 6.5 implied that the complex stoichiometry of Ag^{I}:Yb^{III}:TCAS was 1:1:1 or n:n:n (Supporting Information, Figure S4), where n is an integer that cannot be determined with the method. We next measured the ESI-mass spectrum to determine n = 2 as shown by the main peaks assignable to $Ag^{I}_{2}\cdot Yb^{III}_{2}\cdot TCAS_{2}$: $[2Ag^{+} + 2Yb^{3+} + 2TCAS^{8-} + 5H^{+}]^{3-}$, m/z = 728.0803(obs.), 728.0792(calcd.) (Figures 4 and Supporting Information, Figure S5). An attempt was made to measure the molar ratio at high pH (= 9.5); however, this attempt failed because of concomitant formation of the Ag^{I}-TCAS and Yb^{III}-TCAS binary complexes. Despite this, ESI-MS clarified the formation

dx.doi.org/10.1021/ic2019583 | Inorg. Chem. 2012, 51, 1648−1656

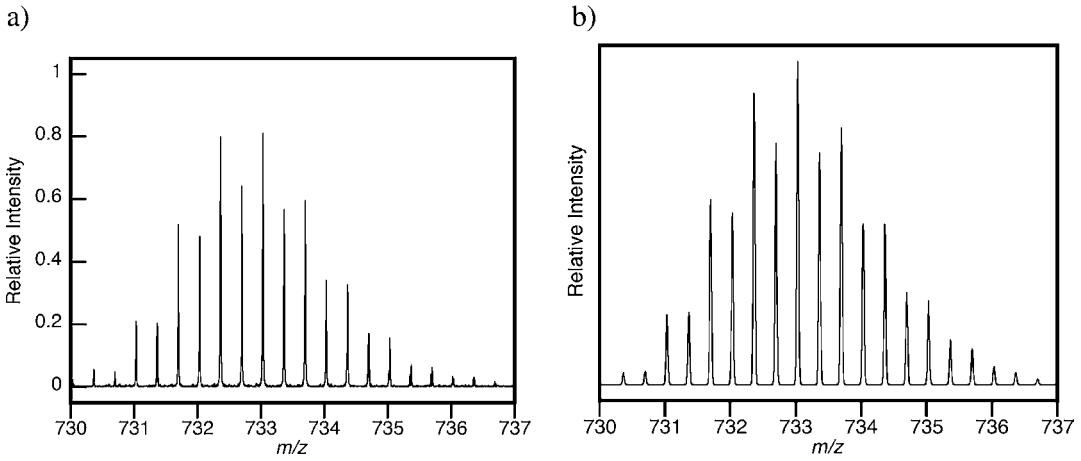

Figure 3. ESI-mass spectra of Ag^{I}-Nd^{III}-TCAS ternary system for $[4Ag^{+} + Nd^{3+} + 2TCAS^{8-} + 6H^{+}]^{3-}$ part. (a) $[Nd^{III}] = 4.0 \times 10^{-5}$ M, $[Ag^{I}] = 1.6 \times 10^{-4}$ M, [TCAS] = 8.0×10^{-5} M, pH 5.9 (adjusted with NH_3), (b) simulation.

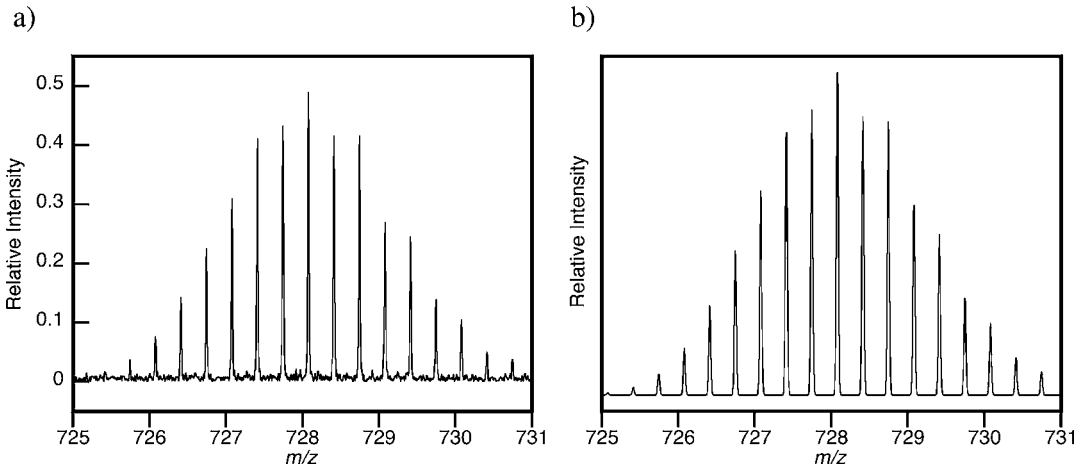

Figure 4. ESI-mass spectra of Ag^{I}-Yb^{III}-TCAS ternary system for $[2Ag^{+} + 2Yb^{3+} + 2TCAS^{8-} + 5H^{+}]^{3-}$ part (pH 6.5). (a) $[Yb^{III}] = 8.0 \times 10^{-5}$ M, $[Ag^{I}] = 8.0 \times 10^{-5}$ M, [TCAS] = 8.0×10^{-5} M, pH 6.5 (adjusted with NH_3), (b) simulation.

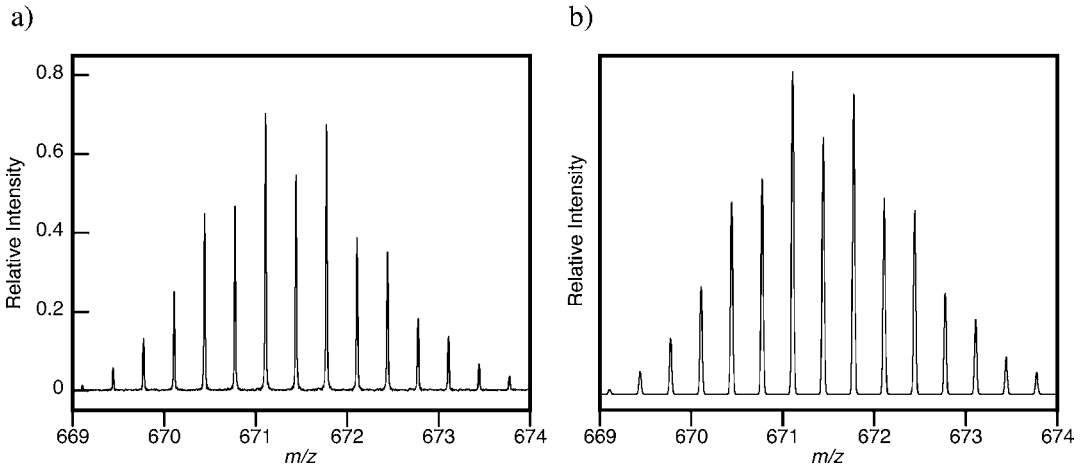

Figure 5. ESI-mass spectra of Ag^{I}-Yb^{III}-TCAS ternary system for $[2Ag^{+} + Yb^{3+} + 2TCAS^{8-} + 8H^{+}]^{3-}$ part (pH 9.5). $[Yb^{III}] = 4.0 \times 10^{-5}$ M, $[Ag^{I}] = 8.0 \times 10^{-5}$ M, [TCAS] = 8.0×10^{-5} M, pH 9.5 (adjusted with NH_3), b) simulation.

of $Ag^{I}_2 \cdot Yb^{III} \cdot TCAS_2$ ($[2Ag^{+} + Yb^{3+} + 2TCAS^{8-} + 7H^{+}]^{4-}$, m/z = 503.0800(obs.), 503.0797(calcd.) and $[2Ag^{+} + Yb^{3+} + 2TCAS^{8-} + 8H^{+}]^{3-}$, m/z = 671.1098(obs.), 671.1088(calcd.) (Figures 5 and Supporting Information, Figure S6). Thus, these results confirmed that the Yb^{III} system gave $Ag^{I}_2 \cdot Yb^{III}_2 \cdot TCAS_2$ at lower pH and $Ag^{I}_2 \cdot Yb^{III} \cdot TCAS_2$ at higher pH. This should lead to the two-step increase in luminescence intensity shown in Figure 2b, as in the case of the Ag^{I}-Tb^{III}-TCAS system.[11] The common features of the complex stoichiometry as well as the two-step formation of $Ag^{I}_2 \cdot Ln^{III}_2 \cdot TCAS_2$ and then

dx.doi.org/10.1021/ic2019583 | Inorg. Chem. 2012, 51, 1648–1656

Ag^{I}_{2}·Ln^{III}·$TCAS_2$ while increasing the pH strongly suggest that both the Yb^{III} and Tb^{III} complexes have the same structures as those shown in Schemes 1 and 2. Namely, in Ag^{I}_{2}·Yb^{III}_{2}·$TCAS_2$, the TCAS ligands sandwich the Ag_2Yb_2 core arranged in a Ag−Ag−Yb−Yb cyclic array, in which each Yb^{III} is coordinated by both O^- and S donor atoms (Scheme 2).[25] Conversely, in Ag^{I}_{2}·Ln^{III}·$TCAS_2$, the TCAS ligands sandwich the Ag_2Yb core, in which Yb^{III} is accommodated in the O_8 cube of the phenolate O^- (Scheme 1).

In summary, the Ag^{I}-Nd^{III}-TCAS system yielded Ag^{I}_{4}·Nd^{III}·$TCAS_2$ in a wide pH range, whereas the Ag^{I}-Yb^{III}-TCAS system behaved very similarly to the Ag^{I}-Tb^{III}-TCAS system, giving Ag^{I}_{2}·Yb^{III}_{2}·$TCAS_2$ at lower pH and Ag^{I}_{2}·Yb^{III}·$TCAS_2$ at higher pH. The similarity of the Yb^{III} and Tb^{III} complexes can be rationalized by the fact that there is only a slight difference in the ionic radii of Yb^{III} (1.125 Å for coordination number (C.N.) = 8) and Tb^{III} (1.180 Å for C.N. = 8) ions.[26] It is important to note that the Nd^{III} and Yb^{III} systems differed, which leads to a question as to how the outcome of the Ag^{I}-Ln^{III}-TCAS system is affected by the Ln^{III} species. Although a systematic study dealing with all members of the Ln^{III} series should be conducted to investigate the behavior leading to formation of the ternary complex, the preliminary results of a study of a Ag^{I}-Gd^{III}-TCAS system suggest a dependence on ionic radii (r). For example, at pH 6.0, ESI-MS analysis of the ternary mixture revealed a principal peak that could be assigned to Ag^{I}_{2}·Gd^{III}_{2}·$TCAS_2$ ($[2Ag^+ + 2Gd^{3+} + 2TCAS^{8-} + 4H^+]^{4-}$; m/z = 537.8002(obs.), 537.8034(calcd.)), revealing similarity to Tb^{III} and Yb^{III} systems. In contrast, at pH 10.0, the Ag^{I}-Gd^{III}-TCAS system produced a main peak for Ag^{I}_{4}·Gd^{III}·$TCAS_2$ ($[4Ag^+ + Gd^{3+} + 2TCAS^{8-} + 4H^+]^{5-}$; m/z = 441.6149(obs.), 441.6148(calcd.)), demonstrating similarity to the Nd^{III} system. Thus, the reactions can be described as follows. First, large Ln^{III} such as Nd^{III} (r = 1.249 Å for C.N. 8[26]) formed a ternary complex, Ag^{I}_{4}·Ln^{III}·$TCAS_2$, at slightly acidic to basic pH. Second, Ln^{III} smaller than Tb^{III} formed Ag^{I}_{2}·Ln^{III}_{2}·$TCAS_2$ at lower pH and Ag^{I}_{2}·Ln^{III}·$TCAS_2$ at higher pH. Third, Gd^{III} (r = 1.193 Å for C.N. 8[26]) was about the size of the boundary to have behaved like Tb^{III} to form Ag^{I}_{2}·Ln^{III}_{2}·$TCAS_2$ at lower pH and like Nd^{III} to form Ag^{I}_{4}·Ln^{III}·$TCAS_2$ at higher pH. As discussed later, the large ionic radius of Nd^{III} should ease the crowded coordination environment of the Ag_4Ln pentametal core to allow assembly. Conversely, the smaller Ln^{III} cannot afford the crowded Ag_4Ln assembly to produce an Ag_2Ln trimetal core at higher pH and an Ag_2Ln_2 tetrametal core at lower pH.

The stoichiometry of Ln^{III} to TCAS for the binary systems was also confirmed to be 1:1 based on the molar ratio and ESI-MS (Supporting Information, Figures S7−S9). By analogy to the manner of coordination of TCAS in the Tb^{III}·TCAS complex,[10] TCAS should coordinate to the Nd^{III} and Yb^{III} centers by ligation with the O^-,S,O^- donor atom sets (Scheme 2). Because of the unsaturated coordination environment of Ln^{III}, it should accept coordinating water molecules, the number (q) of which should be about 5 assuming C.N. = 8 and was estimated to be 4.8 for Tb^{III}.[11]

X-ray Structure of the Nd^{III} Complex. To clarify the three-dimensional structure of the ternary complexes, we attempted to isolate single crystals for Ag^{I}_{4}·Nd^{III}·$TCAS_2$, Ag^{I}_{2}·Yb^{III}_{2}·$TCAS_2$, and Ag^{I}_{2}·Yb^{III}·$TCAS_2$ from aqueous solutions. As a result, slow diffusion of DMF vapor into an aqueous solution containing Ag^{I}, Nd^{III}, and TCAS in a ratio of 4:1:2 successfully produced crystals of Ag^{I}_{4}·Nd^{III}·$TCAS_2$ with sufficient quality for X-ray analysis (Figure 6). Two TCAS ligands were found to sandwich the Ag_4Nd metal core by providing all of its O_4S_4 donor atoms, resulting in a double-cone structure. The three-dimensional structure of the complex appeared to be isostructural to the Ag^{I}_{4}·Tb^{III}·$TCAS_2$,[12] causing it to have the same characteristic features. For example, the two TCAS ligands were bridged by four S−Ag^{I}−S linkages to provide an Nd^{III} center with an almost exact O_8-cubic coordination environment (Figure 7), which is one of the rare examples of coordination geometries having sterically less favorable orientation owing to ligand−ligand repulsion.[12,27,28] Moreover, the complex seemingly had D_{4h} symmetry with a 4-fold axis passing through the Nd^{III} and center of the cone-shaped TCAS. However, since the TCAS ligands distorted from an ideal cone to a pinched-cone conformation, the complex actually has C_i symmetry with the inversion center at the Nd^{III}.

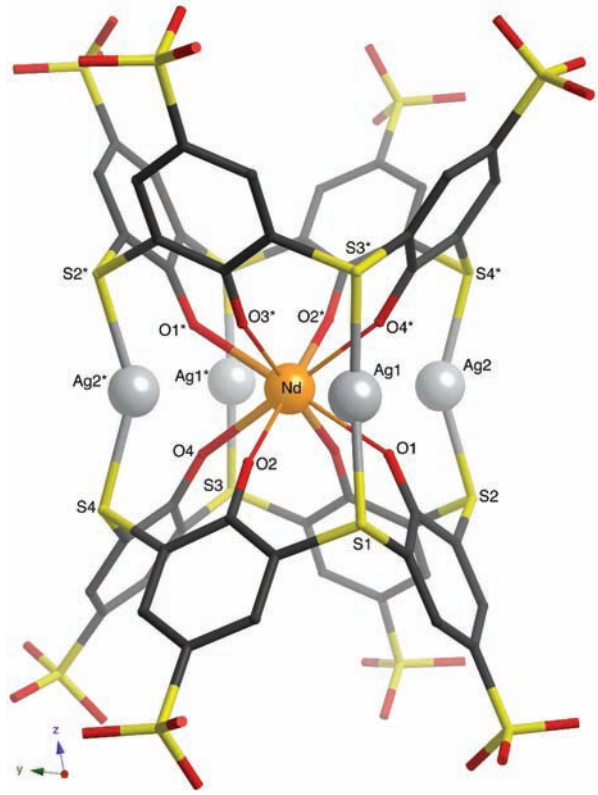

Figure 6. X-ray structure of Ag^{I}_{4}·Nd^{III}·$TCAS_2$ complex viewing along the x-axis of the unit cell. Nd^{III} is located at the crystallographic inversion center and half of the molecule is independent.

Scrutiny of the crystal structure of Ag^{I}_{4}·Nd^{III}·$TCAS_2$ revealed subtle but distinct differences from that of Ag^{I}_{4}·Tb^{III}·$TCAS_2$ arising from differences in the ionic radii between Nd^{III} and Tb^{III} (0.07 Å for C.N. 8).[26] First, the O_8 cube was slightly enlarged, and the average distance of the adjacent O−O in the TCAS ligand forming the basal square of the cube in Ag^{I}_{4}·Nd^{III}·$TCAS_2$ was 2.895(2) Å (Supporting Information, Table S1). This distance was about 0.05 Å longer than that of its Tb^{III} counterpart (2.844(4) Å), suggesting that the Nd^{III} pushed the O^- donor atoms to widen the square. In contrast, the interligand O−O distance corresponding to the length of the height of the cube of Ag^{I}_{4}·Nd^{III}·$TCAS_2$ was 2.680(2) Å, which was only about 0.01 Å longer than that of Ag^{I}_{4}·Tb^{III}·$TCAS_2$ (2.667(4) Å). Thus, the shape of the cube

dx.doi.org/10.1021/ic2019583 | Inorg. Chem. 2012, 51, 1648−1656

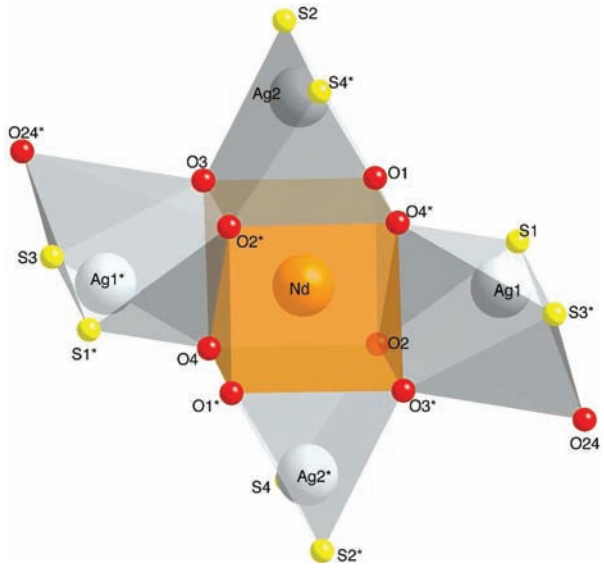

Figure 7. Coordination environment of the Ag_4Nd core. Selected bond length [Å]: Nd1–O1 2.5234(14), Nd1–O2 2.4087(15), Nd1–O3 2.4381(15), Nd1–O4 2.4143(14), O1–Ag2 2.5972(15), Ag1–S1 2.4628(5), Ag1–S3 2.4590(5), Ag2–S2 2.4453(5), Ag2–S4 2.4293(5).

became slightly wider in response to replacement of Tb^{III} with Nd^{III} owing to the ionic radius being 0.07 Å larger. Second, the interligand distances increased by 0.04 Å based on the S–S distance between the two facing TCAS ligands, which were 4.719(1) and 4.683(2) Å for the Nd^{III} and Tb^{III} complexes, respectively. These findings also indicate that the slightly larger Nd^{III} caused the two calixarenes to separate. Third, the Ag–Ln and Ag–Ag intermetal distances in Nd^{III} were 0.03 and 0.04 Å longer than those in Tb^{III}. This can be explained as follows: moving the two calix ligands away from each other causes the Ag^{I} ion suspended by the S–Ag–S bridge between the two TCAS to depart from the center (i.e., Nd^{III} ion) of the complex. This is also indicated by the fact that the angle of the S–Ag–S bridge in $Ag^{I}_4{\cdot}Nd^{III}{\cdot}TCAS_2$ was 1.46° larger than that of $Ag^{I}_4{\cdot}Tb^{III}{\cdot}TCAS_2$. Fourth, the dihedral angle between the distal phenyl rings in the calix[4]arene ring in $Ag^{I}_4{\cdot}Nd^{III}{\cdot}TCAS_2$ was about 0.5° smaller than those of $Ag^{I}_4{\cdot}Tb^{III}{\cdot}TCAS_2$, suggesting that the large Nd^{III} ion pushes the oxygen atom, causing the phenol ring to stand with respect to the plane consisting of the four S atoms of the TCAS. Overall, the large Nd^{III} ion causes the coordination environment of the Ag_4Ln heterometal core to be slightly less crowded, which should ease the electrostatic and steric repulsion and increase stability. This should allow formation of the ternary complex $Ag^{I}_4{\cdot}Nd^{III}{\cdot}TCAS_2$ in aqueous solution at a wide pH range, which cannot be afforded by Tb^{III} and Yb^{III} ions smaller than Nd^{III}.

From the viewpoint of designing the ligand for lanthanide complexes with efficient NIR emission, it should be noted that the O_8-cubic geometry in the spontaneously formed $Ag^{I}_4{\cdot}Nd^{III}{\cdot}TCAS_2$ successfully excluded quenchable water molecules from the first coordination shell (Figure 7). This enabled circumvention of the elaborate synthesis of the ligand as exemplified by **1** and **2**. The key factor in the spontaneous formation of $Ag^{I}_4{\cdot}Nd^{III}{\cdot}TCAS_2$ should be the sharp selectivity of the donor atoms of TCAS toward metal ions. Specifically, soft S coordinates to soft Ag^{I} and hard O^{-} coordinates to hard Nd^{III}. This makes it possible to heterogeneously assemble the heterometal core while maintaining precise positioning of metal ions in the complex. The Nd^{III} ion sits in the center of the cage to serve as a luminescent center, while the four Ag^{I} ions exist around the periphery of the Nd^{III} center to support the cage structure (Figure 6).

Photophysical Properties. Here, we examine whether the luminescence quantum efficiency (Φ) of the ternary complexes is larger than that of the binary complexes in aqueous solutions. The Φ value was determined as previously described[10] using Nd^{III}- and Yb^{III}-calcein complexes as the standard[16] (Table 1). The ternary systems gave larger Φ values than the binary systems did. For example, the quantum efficiency of

Table 1. Molar Absorption Coefficient (ε) at the Excitation Wavelength (λ_{ex}) and Overall Luminescence Quantum Yield (Φ) for the Complexes

complex	pH	ε /$M^{-1}cm^{-1}$[a]	λ_{ex}/nm	Φ[b]
Nd·TCAS	9.1	22500	315	8.2×10^{-5}[c]
Ag_4·Nd·$TCAS_2$	5.9	35500	312	4.9×10^{-4}
Nd·Calcein	8.3	72300	500	1.7×10^{-4}[d]
Yb·TCAS	9.0	20500	313	2.0×10^{-4}[c]
Ag_2·Yb_2·$TCAS_2$	6.5	41400	318	3.8×10^{-4}
Ag_2·Yb·$TCAS_2$	9.5	34800	312	3.3×10^{-3}
Yb·Calcein	8.3	92900	500	8.9×10^{-4}[d]

[a]The ε value at λ_{ex}. [b]The Φ value was determined under aerated conditions unless otherwise noted. [c]Determined under N_2 atmosphere. [d]Reported standard value. See reference 16.

$Ag^{I}_4{\cdot}Nd^{III}{\cdot}TCAS_2$ was determined to be $\Phi = 4.9 \times 10^{-4}$ (in H_2O), which was about six times larger than that of the $Nd^{III}{\cdot}TCAS$ complex ($\Phi = 8.2 \times 10^{-5}$ in H_2O). Although the sensitization efficiency (the product of the efficiencies in the processes of $S_1 \rightarrow T_1$ intersystem crossing at the TCAS ligand and energy transfer from TCAS to Nd^{III}) should differ among $Ag^{I}_4{\cdot}Nd^{III}{\cdot}TCAS_2$ and $Nd^{III}{\cdot}TCAS$ complexes, the water-free coordination environment of the former exemplified by the solid state structure (Figure 7) appears to be responsible for the higher quantum efficiency. In fact, in aqueous solution, the number of water molecules coordinating to Nd^{III} was estimated[17] to be nearly zero (Table 2). Obviously, the q value for $Nd^{III}{\cdot}TCAS$ should not differ greatly from that for $Tb^{III}{\cdot}TCAS$ (i.e., q = 4.8,[11] see Scheme 2). Accordingly, the

Table 2. Emission Lifetime (τ) and the Number of Coordinated Water Molecules (q) to Ln^{III} in the Ternary Complexes[a]

complex	pH	$\tau_{H2O}/\mu s$	$\tau_{D2O}/\mu s$	q
Ag_4·Nd·$TCAS_2$	5.9	0.48	3.85	−0.16
Ag_2·Yb_2·$TCAS_2$	6.5	0.37	11.9	2.40
Ag_2·Yb·$TCAS_2$	9.5	4.35	12.0	− 0.05

[a]Determined under aerated conditions.

steep difference in the absence and presence of the O–H oscillation at the first coordination sphere of Nd^{III} should lead to a large difference in the Φ value of the ternary and binary complexes.

As mentioned in the Introduction, the quantum yield of NIR-emissive lanthanide complexes are generally small (~10^{-4} for Nd^{III} in H_2O),[3] and the highest one to date was obtained with $Nd^{III}_2{\cdot}$**1** (see Scheme 1 for the photophysical properties).[5]

dx.doi.org/10.1021/ic2019583 | Inorg. Chem. 2012, 51, 1648–1656

The luminescence quantum yield of $Ag^{I}_{4}{\cdot}Nd^{III}{\cdot}TCAS_2$ was more than half that of complex $Nd^{III}{}_2{\cdot}\mathbf{1}$ and larger than $Nd^{III}{\cdot}\mathbf{2}$[6] (Scheme 1). To the best of our knowledge, $Ag^{I}_{4}{\cdot}Nd^{III}{\cdot}TCAS_2$ provides the second largest Φ value in water that has been reported to date. In addition, we investigated the effects of N_2 and O_2 gases saturated in the ternary complex solutions on the Φ value to determine the $T_1 \rightarrow Ln^{III}$ efficiency because dissolved O_2 easily quenches the T_1-excited state (Table 3). After the solution of $Ag^{I}_{4}{\cdot}Nd^{III}{\cdot}TCAS_2$ was saturated with N_2, the Φ value only increased by about 12%. Conversely,

Table 3. Effect of N_2 and O_2 Saturation on the Luminescence Quantum Yield (Φ)

complex	air	N_2 atmosphere	O_2 atmosphere
$Ag_4{\cdot}Nd{\cdot}TCAS_2$	4.9×10^{-4}	5.5×10^{-4}	4.8×10^{-4}
$Ag_2{\cdot}Yb{\cdot}TCAS_2$	3.3×10^{-3}	3.6×10^{-3}	3.1×10^{-3}

saturation with O_2 led to a slight decrease in the Φ value, suggesting that the efficiency of $T_1 \rightarrow Nd^{III}$ energy transfer is sufficient to be insensitive to quenching of the T_1 state with O_2. This also contributes to the large Φ value of $Ag^{I}_{4}{\cdot}Nd^{III}{\cdot}TCAS_2$.

For the ternary Yb^{III} complexes, the number of coordinating water molecules, q, was also determined (Table 2) to rationalize the proposed structures of $Ag^{I}_{2}{\cdot}Yb^{III}{}_2{\cdot}TCAS_2$ (Scheme 2) and $Ag^{I}_{2}{\cdot}Yb^{III}{\cdot}TCAS_2$ (Scheme 1). For example, the Yb^{III} center of $Ag^{I}_{2}{\cdot}Yb^{III}{}_2{\cdot}TCAS_2$ in the proposed structure should have two or three water molecules assuming that the C.N. of Yb^{III} is 8 or 9, respectively, which agrees with the measured q value in the middle of the proposed value. For $Ag^{I}_{2}{\cdot}Yb^{III}{\cdot}TCAS_2$, Yb^{III} is accommodated in the O_8 cube of eight phenolate O^- groups to give $q = 0$. The Φ value for the Yb^{III} complexes varies in the order of $Yb^{III}{\cdot}TCAS < Ag^{I}_{2}{\cdot}Yb^{III}{}_2{\cdot}TCAS_2 < Ag^{I}_{2}{\cdot}Yb^{III}{\cdot}TCAS_2$ (Table 1), which seems to be related to the number of q. For example, $Ag^{I}_{2}{\cdot}Yb^{III}{\cdot}TCAS_2$ with no coordinating water molecules ($q = 0$) was found to have the highest Φ value. These findings clearly indicate that the exclusion of water molecules is of key importance in the design of highly efficient NIR-emissive lanthanide complexes. In fact, the Φ value of $Ag^{I}_{2}{\cdot}Yb^{III}{\cdot}TCAS_2$ was only slightly smaller than those obtained with complexes $Yb^{III}{}_2{\cdot}\mathbf{1}$[5] and $Yb^{III}{\cdot}\mathbf{2}$[6] in H_2O (Scheme 1). Considering the other factors, such as the simple design, ease in the preparation, and beauty of the structure, $Ag^{I}_{2}{\cdot}Yb^{III}{\cdot}TCAS_2$ should be more attractive than $Yb^{III}{}_2{\cdot}\mathbf{1}$ and $Yb^{III}{\cdot}\mathbf{2}$. In addition, the high efficiency in the $T_1 \rightarrow Yb^{III}$ energy transfer in $Ag^{I}_{2}{\cdot}Yb^{III}{\cdot}TCAS_2$ demonstrated by the lack of sensitivity of the Φ value to the O_2 concentration in the solution (Table 3) appears to facilitate the high overall luminescence quantum yield.

As exemplified by $Ag^{I}_{4}{\cdot}Nd^{III}{\cdot}TCAS_2$ and $Ag^{I}_{2}{\cdot}Yb^{III}{\cdot}TCAS_2$, simply mixing the components such as the bridging Ag^{I}, luminescent center Ln^{III}, and antenna-ligand TCAS successfully provided the ternary complexes with superb photophysical properties. These properties arose from ejection of the coordinating water molecules from the Ln^{III} center by accommodation in the O_8-cubic coordination environment. These findings confirm the effectiveness of the noncovalent strategy for the NIR-emissive complex via one-step heterometal assembly by designing simple molecules with donor atoms that have sharp selectivity toward the metal ions. Recently, strategies used to obtain NIR-emissive Ln^{III} complex via heterometal assembly rather than relying on covalent connection of multidentate ligands with chromophores have been reported.[13] For example, Piguet and Bünzli et al. reported triple helical complexes including a d-block metal ion (M) and Ln^{III},[29] which enabled fine-tuning of photophysical properties such as the NIR-luminescence lifetime.[30] The design of the complex is based on ligands consisting of Ln^{III}- and M-binding segments, the latter of which binds to M to form a tripodal spacer for binding to Ln^{III} to shield in a tricapped trigonal-prism coordination environment. However, when compared to our ternary complex, their triple-helical approach still requires programming of the self-assembly processes via careful design of the ligand as well as multistep synthesis to construct the segmental structure. These findings highlight the simplicity of our $Ag^{I}_{4}{\cdot}Nd^{III}{\cdot}TCAS_2$ and $Ag^{I}_{2}{\cdot}Yb^{III}{\cdot}TCAS_2$, in which no segments are found.

CONCLUSION

In conclusion, simply mixing the ternary components in aqueous solutions led to heterogeneous self-assembly of $Ag^{I}_{4}{\cdot}Nd^{III}{\cdot}TCAS_2$ and $Ag^{I}_{2}{\cdot}Yb^{III}{\cdot}TCAS_2$, which emit highly efficient NIR light owing to the cage structure providing an Ln^{III} center that enables the O_8-cubic coordination environment to expel quenchable water molecules. The crystallographic structure of $Ag^{I}_{4}{\cdot}Nd^{III}{\cdot}TCAS_2$ clearly demonstrated that the key to the water-free O_8-cubic environment was the ability of the O_4S_4 donor atoms of TCAS to selectively allow Ag^{I} to bridge the two TCAS ligands with S−Ag^{I}−S linkages to form the cage structure. Thus, this study inspired the use of a noncovalent strategy to rationally design a ligand for an NIR-emissive Ln^{III} complex to encapsulate the Ln^{III} core in a cage structure supported by coordination linkages with the aid of an auxiliary metal ion. This should be a highly powerful alternative to ligand design that rely on covalent joining of multidentate ligand(s) with chromophores that require multistep synthesis. Studies to develop a method of conjugating $Ag^{I}_{4}{\cdot}Nd^{III}{\cdot}TCAS_2$ and $Ag^{I}_{2}{\cdot}Yb^{III}{\cdot}TCAS_2$ to biomolecules are now underway with the ultimate goal of their application to bioassay and NIR imaging.

ASSOCIATED CONTENT

Supporting Information

X-ray crystallographic data for $Ag^{I}_{4}{\cdot}Nd^{III}{\cdot}TCAS_2$ in CIF format. The molar ratio plots (Figures S1, S4, and S7), electro-spray ionization-mass spectra (Figures S2, S3, S5, S6, and S8−S11), emission decay curves (Figures S12−S14), time dependence of absorbance of the complex solutions (Figure S15), selected interatomic distances and angles of $Ag^{I}_{4}{\cdot}Nd^{III}{\cdot}TCAS_2$ (Table S1), and estimated decay constants (Table S2). This material is available free of charge via the Internet at http://pubs.acs.org.

AUTHOR INFORMATION

Corresponding Author

*E-mail: iki@m.tohoku.ac.jp. Fax: +81-22-795-7293.

ACKNOWLEDGMENTS

This study was supported by Grants-in-Aid from Japan Society of the Promotion of Science (JSPS) [Nos. 20350070 and 23655060]. We also thank Profs. H. Tsukube and S. Shinoda for their kind assistance with measurement of the luminescence lifetime of the complexes.

REFERENCES

(1) Nagano, T. *Proc. Jpn. Acad., Ser. B* **2010**, *86*, 837−847.
(2) Achilefu, S. *Angew. Chem., Int. Ed.* **2010**, *49*, 9816−9818.

(3) Comby, S., Bünzli, J.-C. G. In *Handbook on the Physics and Chemistry of Rare Earth*; Gschneidner, K. A., Bünzli, J.-C. G., Pecharsky, V. K., Eds.; Elsevier: Amsterdam, The Netherlands, 2007; Vol. *37*, pp 217−470.
(4) Eliseeva, S. V.; Bünzli, J. C. G. *Chem. Soc. Rev.* **2010**, *39*, 189−227.
(5) Korovin, Y. V.; Rusakova, N. V.; Popkov, Y. A.; Dotsenko, V. P. *J. Appl. Spectrosc.* **2002**, *69*, 841−844.
(6) Comby, S.; Imbert, D.; Chauvin, A.-S.; Bünzli, J.-C. G. *Inorg. Chem.* **2006**, *45*, 732−743.
(7) Iki, N.; Kabuto, C.; Fukushima, T.; Kumagai, H.; Takeya, H.; Miyanari, S.; Miyashi, T.; Miyano, S. *Tetrahedron* **2000**, *56*, 1437−1443.
(8) Morohashi, N.; Narumi, F.; Iki, N.; Hattori, T.; Miyano, S. *Chem. Rev.* **2006**, *106*, 5291−5316.
(9) Iki, N.; Fujimoto, T.; Miyano, S. *Chem. Lett.* **1998**, *27*, 625−626.
(10) Iki, N.; Horiuchi, T.; Oka, H.; Koyama, K.; Morohashi, N.; Kabuto, C.; Miyano, S. *J. Chem. Soc., Perkin Trans.* **2001**, *2*, 2219−2225.
(11) Iki, N.; Ohta, M.; Horiuchi, T.; Hoshino, H. *Chem.—Asian J.* **2008**, *3*, 849−853.
(12) Tanaka, T.; Iki, N.; Kajiwara, T.; Yamashita, M.; Hoshino, H. *J. Inclusion Phenom. Macrocyclic Chem.* **2009**, *64*, 379−383.
(13) Iki, N. *Supramol. Chem.* **2011**, *23*, 160−168.
(14) Ueno, K. *Chelatometry*; Nankodo: Tokyo, Japan, 1989.
(15) Roethlisberger, U. *iMass for Mac OS X*; 2002
(16) Werts, M. H. V.; Verhoeven, J. W.; Hofstraat, J. W. *J. Chem. Soc., Perkin Trans.* **2000**, *2*, 433−439.
(17) Faulkner, S.; Beeby, A.; Carrie, M.-C.; Dadabhoy, A.; Kenwright, A. M.; Sammes, P. G. *Inorg. Chem. Commun.* **2001**, *4*, 187−190.
(18) Beeby, A.; Clarkson, I. M.; Dickins, R. S.; Faulkner, S.; Parker, D.; Royle, L.; de Sousa, A S.; Williams, J. A. G.; Woods, M. *J. Chem. Soc., Perkin Trans.* **1999**, *2*, 493−504.
(19) Sheldrick, G. M. *SHELXS-97, Programs for Crystal Structure Analysis*; University of Göttingen: Göttingen, Germany, 1998.
(20) Sheldrick, G. M. *Acta Crystallogr., Sect. A* **2008**, *64*, 112−122.
(21) Kabuto, C.; Akine, S.; Nemoto, T.; Kwon, E. *J. Cryst. Soc. Jpn.* **2009**, *51*, 218−224.
(22) Bünzli, J.-C. G. *Luminescent Probes*; Elsevier: Amsterdam, The Netherlands, 1989.
(23) Yanagida, S.; Hasegawa, Y.; Wada, Y. *J. Lumin.* **2000**, *87*−*89*, 995−998.
(24) Puntus, L. N.; Zolin, V. F.; Babushkina, T. A.; Kutuza, I. B. *J. Alloys Compd.* **2004**, *380*, 310−314.
(25) For Tb(III), see Tanaka, T.; Iki, N., Hoshino, H.; unpublished results, Tohoku University, 2009.
(26) Shannon, R. *Acta Crystallogr., Sect. A* **1976**, *32*, 751−767.
(27) Cotton, F. A., Wilkinson, G. *Advanced Inorganic Chemistry*, 5th ed.; John Wiley & Sons: New York, 1988.
(28) Haigh, C. W. *Polyhedron* **1996**, *15*, 605−643.
(29) Piguet, C., Bünzli, J.-C. G. In *Handbook on the Physics and Chemistry of Rare Earths*; Gschneidner, J. K. A., Bünzli, J.-C. G., Pecharsky, V. K., Eds.; Elsevier: Amsterdam, The Netherlands, 2010; Vol. *40*, pp 301−553.
(30) Torelli, S.; Imbert, D.; Cantuel, M.; Bernardinelli, G.; Delahaye, S.; Hauser, A.; Bünzli, J.-C. G.; Piguet, C. *Chem.—Eur. J.* **2005**, *11*, 3228−3242.